

# MATLAS-42, A Globular Cluster-Rich Ultra-Diffuse Galaxy That Diverges from the “Failed Galaxy” Formation Pathway

Jonah S. Gannon<sup>1\*</sup>, Duncan A. Forbes<sup>1</sup>, Francine R. Marleau<sup>2</sup>, Anna Ferré-Mateu<sup>3,4,1</sup>,  
Aaron J. Romanowsky<sup>5,6</sup>, Maria Luisa Buzzo<sup>7,1</sup>, and Jean P. Brodie<sup>1,6</sup>

<sup>1</sup> Centre for Astrophysics and Supercomputing, Swinburne University, John Street, Hawthorn VIC 3122, Australia

<sup>2</sup> Institute für Astro- und Teilchenphysik, Universität Innsbruck, Technikerstraße 25/8, A-6020 Innsbruck, Austria

<sup>3</sup> Instituto de Astrofísica de Canarias, Calle Vía Láctea S/N, E-38205, La Laguna, Tenerife, Spain

<sup>4</sup> Departamento de Astrofísica, Universidad de La Laguna, 38206, La Laguna (S.C. Tenerife), Spain

<sup>5</sup> Department of Physics and Astronomy, San José State University, One Washington Square, San Jose, CA 95192, USA

<sup>6</sup> Department of Astronomy & Astrophysics, University of California Santa Cruz, 1156 High Street, Santa Cruz, CA 95064, USA

<sup>7</sup> Astronomy Department, Yale University, 219 Prospect St, New Haven, CT 06511, USA

Accepted XXX. Received YYY; in original form ZZZ

## ABSTRACT

To date, there has been significant interest in globular cluster (GC)-rich ultra-diffuse galaxies (UDGs) and the evidence that they have formed via an unexpected, “failed galaxy” formation pathway. The majority of the evidence for “failed galaxy” UDGs originates from spectroscopic observations targeting passive GC-rich UDGs, with a focus on those residing in galaxy clusters. In this work, we study the gas-rich, GC-rich group UDG MATLAS-42 and derive its stellar population properties using the Keck Cosmic Web Imager. We measure a redshift for the galaxy ( $V_{R,\star} = 2433 \pm 8 \text{ km s}^{-1}$ ), confirming the previous assumptions that it is both part of the NGC 502 group and has an associated HI-reservoir ( $V_{R,\text{HI}} = 2423 \pm 15 \text{ km s}^{-1}$ ). We measure integrated stellar populations and find the galaxy to be both young (mass-weighted age =  $3.2_{-1.5}^{+2.6}$  Gyr) and of average-to-low metallicity ( $[M/H] = -1.19_{-0.30}^{+0.42}$  dex). When considering these properties in the context of the galaxy’s formation, we note it likely does not follow the “failed galaxy” formation pathway commonly attributed to GC-rich, cluster UDGs, as it has experienced recent star formation. At most it started failed, however, it has recently rejuvenated its star formation. Finally, we build a toy model of the passive evolution of this galaxy, finding that its relative GC-richness (i.e.,  $M_{\text{GC}}/M_{\star}$ ) will likely decrease with time as GCs slowly evaporate/disrupt to contribute to the stellar mass of the galaxy. Due to this, we hypothesise that it is likely not a low redshift analogue of the progenitor to a “failed galaxy” UDGs.

**Key words:** galaxies: dwarf – galaxies: fundamental parameters – galaxies: formation

## 1 INTRODUCTION

Dwarf galaxies are expected to dominate the number density of galaxies in the Universe at all epochs (Wright et al. 2017; Martin et al. 2019) and, as galaxy stellar mass increases, the fraction of stellar mass comprised of accreted dwarf galaxies also increases (see e.g., Remus & Forbes 2022). The advent of deep, wide-area surveys is increasingly finding large numbers of previously overlooked dwarf galaxies. For example, van Dokkum et al. (2015) found 47 large, low surface brightness “ultra-diffuse galaxies” (UDGs) in the Coma cluster. These galaxies were characterised by having large half-light radii ( $> 1.5 \text{ kpc}$ ) and low surface brightnesses ( $\mu_{g,0} > 24 \text{ mag arcsec}^{-2}$ ), which placed them in a region of parameter space that was previously sparsely populated.

Since their discovery, UDGs have been found in all environments, i.e., from the field to massive galaxy clusters, and many large surveys have been conducted to study their formation (e.g., SMUDGs; Zarit-

sky et al. 2019; MATLAS Marleau et al. 2021; LEWIS Iodice et al. 2023; EUCLID-ERO Perseus Marleau et al. 2025). Their study has posed many puzzles that are yet to be solved. Namely, a consensus has yet to be reached as to how they form, with galaxy formation simulations suggesting that stellar feedback (Di Cintio et al. 2017; Chan et al. 2018), higher than average halo spin (Amorisco et al. 2018; Liao et al. 2019), galaxy mergers (Wright et al. 2017), high velocity galaxy collisions (Lee et al. 2021, 2024), ram pressure stripped material (Ivleva et al. 2024), tidal heating and tidal stripping (Carleton et al. 2019; Sales et al. 2020), may be the dominant mechanisms that form UDGs. Combinations of these processes (e.g., Jiang et al. 2019) help to explain the full observed properties of the UDG population (see e.g., Ferré-Mateu et al. 2023).

Crucially, none of the proposed formation pathways that originate from galaxy formation simulations are able to explain how some UDGs are observed to be extremely globular cluster (GC)-rich for their stellar mass (e.g., van Dokkum et al. 2017; Forbes et al. 2020; Danieli et al. 2022; Saifollahi et al. 2022, 2025; Li et al. 2025). In order to create these galaxies, a separate formation pathway, that of a

\* E-mail: jonah.gannon@gmail.com

“failed galaxy” or “pure stellar halo” (van Dokkum et al. 2015; Peng & Lim 2016; Danieli et al. 2022; Forbes & Gannon 2024; Forbes et al. 2025) has been proposed. In this scenario, the UDG forms rapidly at high redshift alongside its GC system. It then quenches and passively evolves until observed today at low redshift. As of yet, no cosmological simulation has found a UDG to follow this pathway; however, their possible properties have been studied using a toy model and the MAGNETICUM simulations (Gannon et al. 2025). Despite their lack of simulated counterparts, there exists myriad evidence for this formation pathway for UDGs:

(i) Their large GC systems (and hence ratio of GC mass to stellar mass;  $M_{GC}/M_{\star}$ ) imply a halo more massive than the stellar mass halo mass relationship (Forbes & Gannon 2024; Forbes & Gannon 2025; Dornan & Harris in press.).

(ii) Many UDG stellar velocity dispersions agree with their residing in massive dark matter halos (Gannon et al. 2022; Zaritsky et al. 2023; Forbes & Gannon 2024). This reinforces the evidence for massive halos from point (i).

(iii) Many UDGs are old, with quick single-burst star formation histories and alpha-enhancement indicative of an early, fast formation (Ferré-Mateu et al. 2018, 2023). A halo evolved through catastrophic quenching and passive stellar evolution from high redshift would help explain its high stellar to halo mass ratios (Gannon et al. 2025).

(iv) Many UDG stellar population gradients are flat with radius, indicative of an “everything everywhere all at once” formation pathway, which is expected for “failed galaxies” (Villaume et al. 2022; Ferré-Mateu et al. 2025). This is likely related to their formation from single burst star formation events (point iii).

(v) Many UDGs in the spectral energy distribution (SED) studies of Buzzo et al. (2024, 2025a) were found to have low metallicities for their stellar mass and to be better aligned with a high redshift mass – metallicity relationship. This helps to confirm their high redshift formation.

(vi) Finally, Buzzo et al. (2025a) used the K-means unsupervised clustering algorithm to assess if multiple populations of UDGs reside in their sample data. They found two populations, with one resembling an extension of normal dwarf galaxies and the other resembling more the properties of “failed galaxy” UDGs. This finding suggests that the “failed galaxy” formation pathway for UDGs is distinct from other dwarf formation mechanisms.

Crucially, however, much of the above evidence for the “failed galaxy” pathway of UDG formation comes from studies which have a known bias to UDGs residing in dense, cluster environments (Gannon et al. 2024b). To further test our understanding of this unique and interesting pathway of galaxy formation, we must increase the sample of GC-rich UDGs in less dense environments.

The MATLAS Survey performed deep, wide-field optical imaging of nearby massive lenticular and elliptical galaxies. Included in their deep imaging are myriad dwarf galaxies, many of which fit the UDG criteria (Habas et al. 2020; Marleau et al. 2021; Poulain et al. 2021). Many of these dwarf galaxies have now received follow-up HI observations (Poulain et al. 2022) and dedicated spectroscopy from MUSE (Müller et al. 2020; Heesters et al. 2023). Of interest to this work is the study of Marleau et al. (2024), which used *Hubble Space Telescope* (HST) imaging of 44 UDGs and 30 NUDGs (Nearly UDGs)<sup>1</sup> in low-density environments to study their GC sys-

<sup>1</sup> Originally this work had 38 UDGs and 36 near UDGs; however, their surface brightnesses have recently been revised in Marleau et al. (Erratum Submitted).

MATLAS-42	
RA [J2000]	20.6260
Dec. [J2000]	+8.7614
$D$ [Mpc]	33.46
Host	NGC 502
$N_{GC}$	$22 \pm 7$
$\log(M_{HI} [M_{\odot}])$	$8.18 \pm 0.06$
$V_{R,HI}$ [km s <sup>-1</sup> ]	$2423 \pm 15$
$m_g$ [mag]	17.46
$R_e$ ["/kpc]	19.44/3.11
$b/a$	0.6
PA [deg]	-43
Sérsic $n$	0.45
$\langle \mu_g \rangle_e$ [mag arcsec <sup>-2</sup> ]	25.94
$\log(M_{\star}/M_{\odot})$	$8.17^{+0.08}_{-0.1}$
$M_{\star}/L_V$	0.97
$V_{R,\star}$ [km s <sup>-1</sup> ]	$2433 \pm 8$
$[M/H]$ [dex]	$-1.19^{+0.42}_{-0.30}$
Age [Gyr]	$3.2^{+2.6}_{-1.5}$

**Table 1.** The key properties of MATLAS-42 from the literature. The properties before the first divide are taken from the MATLAS Survey. In particular, we take data from their online data retrieval tool along with Poulain et al. (2021, 2022) and Marleau et al. (2024). The properties in the middle divide are from the imaging and SED fitting of Buzzo et al. (2024). The properties in the final divide are from this work.

tems. The vast majority of the UDGs they studied (64%) contained few, if any, GCs. Indeed, only a small population, 9%, were found to be particularly GC-rich. One of these UDGs, NGC5846\_UDG1, a.k.a. MATLAS-2019, has already been the target of extensive study due to its rich GC-system (Forbes et al. 2019; Danieli et al. 2022; Müller et al. 2020, 2021; Forbes et al. 2021; Ferré-Mateu et al. 2023; Marleau et al. 2024; Haacke et al. 2025).

Also among the small sample of GC-rich UDGs observed by Marleau et al. (2024) was MATLAS-42. MATLAS-42 is near unique for GC-rich UDGs in that it also has a detection of HI gas, likely to be associated with the galaxy (Poulain et al. 2022). In this work, we perform Keck Cosmic Web Imager (KCWI) spectroscopy of MATLAS-42 to analyse its spectroscopic properties and compare them to the GC-rich UDGs that have been previously studied. A proposed pathway to quench “failed galaxy” UDGs is that feedback from the GC formation ejects the gas, leading to a natural question as to why MATLAS-42 has gas while other GC-rich UDGs do not. We will study how MATLAS-42 may have formed and if it also follows a “failed galaxy” formation pathway despite its location in a lower density environment and its retention of a significant gas reservoir.

In Section 2, we summarise the properties of MATLAS-42 from the literature. We also present our new KCWI observations of the galaxy and the results of these new observations. In Section 3, we discuss the properties of MATLAS-42 in the context of previously spectroscopically observed UDGs and its possible formation pathways. Further, we discuss how MATLAS-42 may evolve in time if left to passive evolution. A brief summary and our conclusions are presented in Section 4. Magnitudes are in the AB system unless otherwise stated. They have been extinction corrected with an extinction of 0.11 in g.

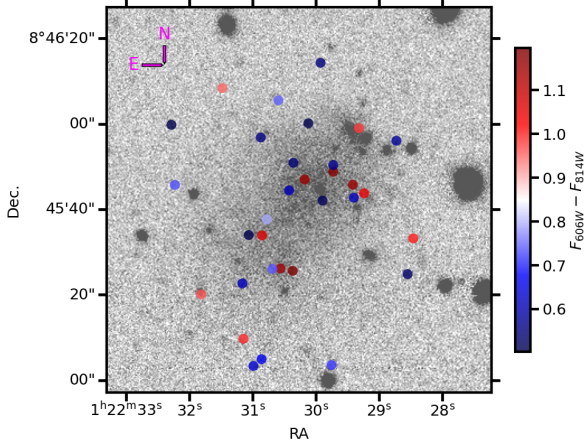


**Figure 1.** The projected distribution of globular cluster candidates around MATLAS-42 on the sky. The cutout is  $1.5 \times 1.5'$  ( $14.6 \times 14.6$  kpc)

Candidates are colour coded by their  $F_{606W} - F_{814W}$  colour from the *HST* imaging of Marleau et al. (2024). North and East are as indicated. The bluer and redder populations of GCs are approximately evenly distributed around the galaxy, with a small extension of both populations coinciding with the irregular extension of MATLAS-42’s stellar body to the south-east.

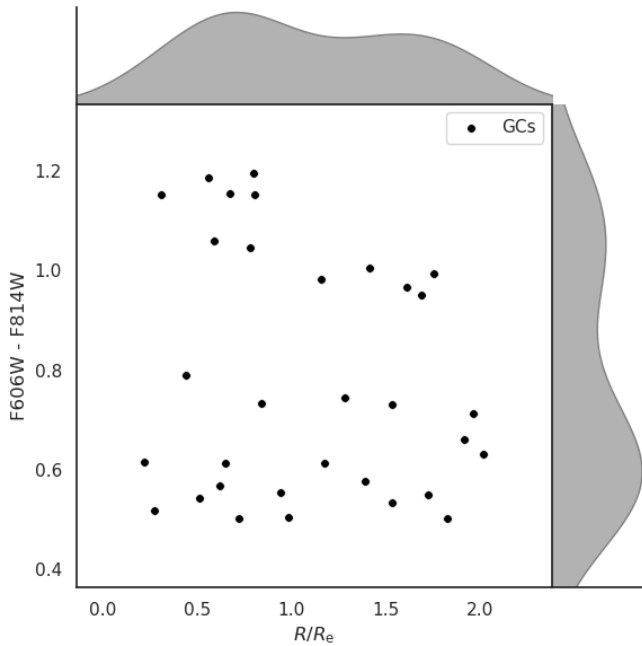


**Figure 2.** GC system candidate colour vs projected radius from the galaxy centre. Kernel density estimates of each axis property are plotted alongside each axis. We take our GC positions and colours from the study of Marleau et al. (2024), which used Vega magnitudes. Note that a significant fraction of the 32 plotted candidates, likely about a third, are statistical contaminants. While GC candidates do not show a strong trend with radius, there is a bimodality in colour.

## 2 MATLAS-42 PROPERTIES AND OBSERVATIONS

In this Section we introduce the properties previously established for MATLAS-42 in the literature and the additions we make to these known properties. We describe the data we gathered and the methods we use to analyse it along with the results of these methods.

### 2.1 Literature

We summarise the key literature properties of MATLAS-42 in Table 1. Much of these data are taken from the MATLAS survey (Marleau et al. 2021). In particular, we have used their online tool<sup>2</sup> to retrieve data, which largely comes from the works of Marleau et al. (2021, 2024) and Poulain et al. (2021, 2022). We additionally take the spectral energy distribution (SED) fitting results for MATLAS-42 from Buzzo et al. (2024), which we will compare to our spectroscopic fitting results later in this work.

A few properties of MATLAS-42 are of particular note for this paper. Namely:

(i) MATLAS-42 has a half-light radius of  $19.44''$  corresponding to  $3.11$  kpc at the assumed distance of the NGC 502/NGC 524 group,  $33.46$  Mpc (Buzzo et al. 2024). Combined with its low surface brightness,  $\langle \mu_g \rangle_e = 25.94$  mag arcsec<sup>-2</sup> (Buzzo et al. 2024), this galaxy is a UDG<sup>3</sup> once the assumption of its distance is verified (as it will be in Section 2.3).

(ii) MATLAS-42 has a total GC system of  $22 \pm 7$  GCs (Marleau et al. 2024, see further for details of methodology on how this total GC estimate was derived). This places it as “GC-rich” under the definition of Gannon et al. (2022), which separates UDGs into GC-rich/GC-poor based on whether they host over/under 20 GCs. The measured GC system of MATLAS-42 corresponds to having a  $M_{GC}/M_\star \approx 2.9\%$  assuming an average GC mass of  $2 \times 10^5 M_\odot$ . This is high fraction of stellar mass in its GC system, atypical for a UDG in a lower density group/field environment (see e.g., Jones et al. 2023), with the majority of GC-rich UDGs thus far being found in galaxy clusters. Having  $\sim 22$  GCs also implies a relatively massive halo mass of  $\log(M_{\text{Halo}}/M_\odot) = 10.87 \pm 14$  (Marleau et al. 2024).

(iii) MATLAS-42 has a coincident HI detection from the ALFALFA survey (Haynes et al. 2018; Poulain et al. 2022), which implies gas associated with the galaxy. The vast majority of UDGs studied spectroscopically thus far are in dense environments and without notable gas content. Furthermore, it is not expected for a dwarf galaxy with high  $M_{GC}/M_\star$  to have significant gas content at late times, as this gas content would likely lead to star formation after the formation of GCs, decreasing its richness relative to its stellar mass.

(iv) It is also of note that MATLAS-42 is both irregular in morphology, with a second stellar component to its south-east (see Figure 1), and has a close companion in MATLAS-41 located to the North West of the UDG (Marleau et al. 2024). The second stellar component is well traced by an extension of the GC candidate population in that direction (see Figure 1/ Figure B1 of Marleau et al. 2024).

(v) The galaxy is slightly bluer than the other UDGs in MATLAS (Marleau et al. 2024), however, it is not extremely blue. There is a hint

<sup>2</sup> [https://matlas.astro.unistra.fr/class/MATLAS\\_dwarfs\\_individual.php?id=MATLAS-42](https://matlas.astro.unistra.fr/class/MATLAS_dwarfs_individual.php?id=MATLAS-42)

<sup>3</sup>  $\langle \mu_g \rangle_e \approx \mu_{g,0} + 1.123$  for  $n = 1$  (Graham & Driver 2005). Hence  $\langle \mu_g \rangle_e = 25.123$  mag arcsec<sup>-2</sup> is approximately the same as  $\mu_{g,0} = 24$  mag arcsec<sup>-2</sup> and thus MATLAS-42 meets the original UDG criteria.



spectral resolution of  $2.52 \text{ \AA}$  (FWHM) which is well-matched to our data and cover a metallicity range of  $-2.27 \leq [M/H] \leq +0.4$  dex and an age range of 0.03 to 14 Gyr. There are 53 steps in age and 12 steps in metallicity, creating 636 distinct combinations of age and metallicity in these models. We fit our data using a 15th-order multiplicative polynomial and a 1st-order additive polynomial to help correct for any flux calibration errors that affect the shape of the galaxy's continuum. Our fitting includes gas templates but does not include pPXF's regularisation parameter, which has been shown to have a negligible effect for UDGs (Ferré-Mateu et al. 2018, 2023). Our fitting included pPXF's cClean parameter to help remove any sky line residuals present in the spectrum (such as those evident near  $5250 \text{ \AA}$ ). After an initial fit, we run 10000 bootstrap fits following the pPXF example `ppxf_example_population_bootstrap.ipynb`<sup>5</sup>. Final stellar population results are quoted from the median of these fits with 16th and 84th percentiles as the uncertainties. Using this process we have measured a mass-weighted age of  $3.2^{+2.6}_{-1.5}$  Gyr and a mass-weighted metallicity  $[M/H] = -1.19^{+0.42}_{-0.30}$  dex. Interestingly, while these results are stable and well-constrained, we were unable to derive a reliable star formation history for MATLAS-42. We discuss this further in Appendix A.

From our initial pPXF fit, we also derive a recessional velocity,  $2433 \pm 8 \text{ km s}^{-1}$ , which has been corrected to the barycentre. We note that this redshift confirms the association of MATLAS-42 with the NGC 502/NGC 524 group ( $2524 \pm 5 \text{ km s}^{-1}$ ; Cappellari et al. 2011) as assumed by both the MATLAS survey and Buzzo et al. (2024). A confirmation of the distance to MATLAS-42 confirms its status as a UDG. It also confirms its association with the HI gas detected in the ALFALFA survey, which has a recessional velocity of  $2423 \pm 15 \text{ km s}^{-1}$  (Poulain et al. 2022), within our stellar recessional velocity's uncertainties. Our stellar population results show that MATLAS-42 is both young and moderately metal-poor, summarised in Table 1. Furthermore, our age and metallicity are in agreement with those from the SED fitting of Buzzo et al. (2024). Their measured metallicity was  $[M/H] = -1.34^{+0.30}_{-0.19}$  dex and their age =  $5.97^{+5.46}_{-3.59}$  Gyr.

Finally, we are also able to fit a recessional velocity for the galaxy included in the offset sky position. Here, we derive a recessional velocity of  $41852 \pm 5 \text{ km s}^{-1}$ . This galaxy is therefore in the background of the group and will not be considered further in this work.

## 3 DISCUSSION

### 3.1 The Mass – Metallicity and Age – Metallicity Relations

In Figure 4, we show the location of MATLAS-42 in the mass – metallicity relationship. The established relationship for classical dwarfs at  $z = 0$  is plotted from Kirby et al. (2013) along with the simulated relationship at  $z = 2.2$  from Ma et al. (2016). We additionally show UDGs from the spectroscopic catalogue of Gannon et al. (2024b)<sup>6</sup>. The plot is colour-coded by the UDG's  $M_{GC}/M_*$  and point styles are per their environment as listed in the Gannon et al. (2024b) catalogue. MATLAS-42 largely follows the  $z = 0$  stellar mass–metallicity relationship, being within the scatter to the metal-poor side. It is less compatible with the relationship at higher redshift. Many UDGs in the spectroscopic catalogue of Gannon et al.

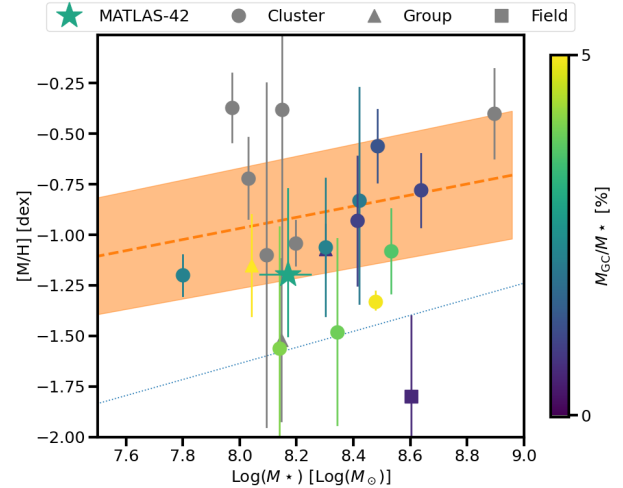


**Figure 4.** The stellar mass–metallicity relationship. We include MATLAS-42 (star) along with UDGs from the catalogue of Gannon et al. (2024b, points) where most come from the study of Ferré-Mateu et al. (2023). The stellar mass – metallicity relationship for classical dwarfs at  $z = 0$  is plotted from Kirby et al. (2013, orange dashed line with  $1-\sigma$  shading) along with the simulated relationship at  $z = 2.2$  from Ma et al. (2016, blue dotted line). Points are colour-coded by their relative GC richness with their style corresponding to their environment (circles are in clusters, triangles are in groups and squares are located in the field). UDGs where no GC count is available are plotted in grey. MATLAS-42 is slightly more metal-poor than the stellar mass – metallicity relationship; however, it is not as metal-poor as the expectation at high redshift. It is a crucial addition to the number of lower-density environment UDGs studied so far.

(2024b), which (for stellar populations) primarily come from the work of Ferré-Mateu et al. (2023), are of similar mass, metallicity and GC richness. MATLAS-42 is unusual, however, as it is in a group environment. The majority of UDGs that have been studied thus far are in a denser, cluster environment. Its stellar populations (mass and metallicity) are most similar to the other UDGs that have been previously studied in a group environment.

In Figure 5 we place MATLAS-42 with the same UDGs in age–metallicity space. While there are a handful of UDGs as young as MATLAS-42, it is overall younger than many of the UDGs that have been studied spectroscopically thus far, including all with measured GC systems. It is worth noting MATLAS-42 is different from other GC-rich UDGs on two fronts. Firstly, it is young and contains gas, as noted above. Secondly, UDGs in lower-density environments are usually found to be GC-poor (Somalwar et al. 2020; Jones et al. 2023).

Given MATLAS-42 still contains significant gas, it is perhaps not unexpected that it hosts a young stellar population. It still leaves a puzzle as to why the other GC-rich UDGs are old and quenched while MATLAS-42 is not. It may be tempting to attribute the early quenching of most of the other UDGs to their being found in a cluster environment. However, it is worth noting that their phase space positioning within clusters does not generally align with the expectation that they were environmentally quenched (Gannon et al. 2022; Forbes et al. 2023). A separate quenching mechanism for at least some of these older UDGs is therefore required, with some attributing it to quenching from feedback as the GC system forms (e.g., Trujillo-Gomez et al. 2022). For MATLAS-42 the implication

<sup>5</sup> [https://github.com/micappe/ppxf\\_examples/blob/main/ppxf\\_example\\_population\\_bootstrap.ipynb](https://github.com/micappe/ppxf_examples/blob/main/ppxf_example_population_bootstrap.ipynb).

<sup>6</sup> Retrieved from [https://github.com/gannonjs/Published\\_Data/tree/main/UDG\\_Spectroscopic\\_Data](https://github.com/gannonjs/Published_Data/tree/main/UDG_Spectroscopic_Data) on January 20th, 2025, see full references in the Data Availability section.

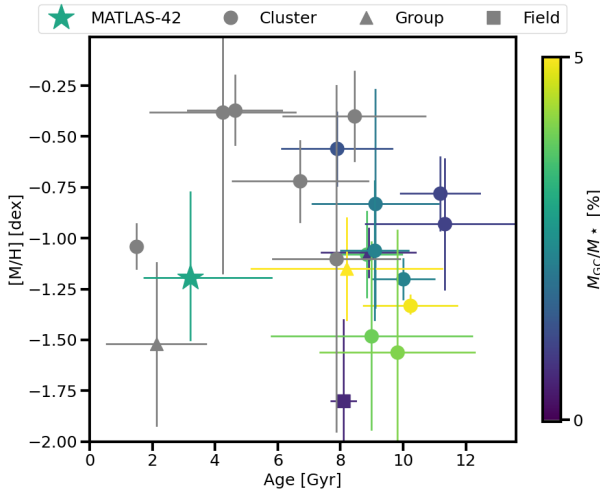


**Figure 5.** Mass-weighted metallicity vs mass-weighted mean stellar age. Point and colour styles follow Figure 4. In comparison to other UDGs known to be GC-rich, MATLAS-42 is noticeably younger. The young age may be attributable to it being in a less-dense group environment, while the other UDGs studied tend to reside in galaxy clusters.

would be that this quenching mechanism was not as permanent as for the other GC-rich UDGs previously studied.

A slightly convoluted explanation for this difference may be that all GC-rich UDGs thus far studied quenched upon the initial GC formation, and the gas ejected from those UDGs now found in dense environments was lost to the galaxy cluster before it could resettle to the centre of its host dark matter halo. In this manner, the quenching time of a GC-rich UDG now found in a galaxy cluster may not exactly match its infall time onto the cluster as its gas was ejected by the GC system’s formation and then was stripped by cluster infall before it was re-accreted. For MATLAS-42, the lack of environmental quenching would allow its gas to settle back into the centre of its halo following its initial ejection at the epoch of GC formation. This gas can form additional stellar mass, furthering the galaxy’s enrichment to its current  $[M/H]$ .

To highlight the unusual properties of MATLAS-42 we can compare it to the four other group and field galaxies in the catalogue of Gannon et al. (2024b), NGC 1052-DF2, NGC5846\_UDG1 (a.k.a., MATLAS-2019), UDG1137+16 and DGSAT I. In comparison to both NGC5846\_UDG1 and DGSAT I, which have a high fraction of their stellar mass in their GC system, MATLAS-42 is  $\sim 5$  Gyr younger than either. We conclude it is unlikely MATLAS-42 has experienced a similar star formation history to either galaxy. Despite this, Janssens et al. (2022) did note a knot of recent star formation within DGSAT I, suggesting that it may be reigniting star formation and may soon be more similar to MATLAS-42 than it is currently, but as a whole, the galaxy is quiescent (Martín-Navarro et al. 2019).

NGC 1052-DF2 is known to exhibit a population of abnormally bright GCs (Shen et al. 2021a) and has been theorised to have formed from a bullet-like collision of dwarf galaxies  $\sim 8$  Gyr ago (Silk 2019; van Dokkum et al. 2022). It is now embedded within a linear trail of galaxies projected on the sky (van Dokkum et al. 2022; Keim et al. 2025; Tang et al. 2025). MATLAS-42 does not exhibit a similar population of bright, monochromatic GCs (Marleau et al. 2024), and while there exist other nearby dwarf companions, MATLAS-41 and MATLAS-43, it is not clear that they follow a linear trail. That

is, MATLAS-42 is not obviously embedded within a linear trail of galaxies on the sky. Given its younger age than NGC 1052-DF2, these galaxies should be much more tightly associated with one another than is seen for the galaxies in the NGC 1052 group. We conclude it is unlikely that MATLAS-42 is another example of this proposed exotic formation pathway.

Finally, when compared to UDG1137+16, MATLAS-42 has a similar age and metallicity. Two differences remain: 1) UDG1137+16 is currently undergoing tidal stripping, although this may not be the cause of its large size (Gannon et al. 2021); 2) UDG1137+16 does not currently have its GC system measured. Given the other dwarf like properties of UDG1137+16 (i.e., its stellar mass, age and metallicity) it seems likely that this galaxy represents a “puffy dwarf” UDG, the tail of the normal dwarf galaxy size – mass distribution to the largest sizes. As MATLAS-42 has a rich GC system, beyond that typically hosted by a dwarf galaxy, it would not easily fit with the picture of a “puffy dwarf”. Based on our comparison to other currently studied field and group UDGs it is not obvious how this galaxy may have formed.

### 3.2 MATLAS-42 Formation

The established formation pathway for many GC-rich UDGs is that of a “failed galaxy” or “pure stellar halo” (van Dokkum et al. 2015; Peng & Lim 2016; Danieli et al. 2022). MATLAS-42 does not fit this formation pathway. Namely, it has not completely failed; its young age suggests that it has recently experienced star formation. Furthermore, it is not necessarily as GC-rich as many of the UDGs that best fit this pathway. For example, NGC 5846\_UDG1 has nearly 13% of its luminosity within its GC system (Danieli et al. 2022, although see Müller et al. 2021 where a number closer to 5% would be derived). It is for this reason that Danieli et al. (2022) suggested that, once you account for the destruction of GCs with time, the galaxy would have had to form nearly its entire stellar mass within its GC system at formation. With  $< 3\%$  of its stellar mass within its GC system, it is very unlikely that the stellar body of MATLAS-42 is entirely/substantially comprised of disrupted GCs. Put another way, while a “failed galaxy”-like formation pathway may have contributed to its initial evolution, it has now diverged from this pathway with subsequent star formation to be something else. This may hint at some level of diversity in evolution following the initial epoch of formation of “failed galaxy” UDGs.

Beyond the failed galaxy formation pathway, it has also been suggested that classical dwarf galaxies may become more GC-rich for their stellar mass in denser environments. This idea is commonly referred to as “biasing” (see e.g., West 1993; Peng et al. 2008). MATLAS-42 is associated NGC 502, which is itself associated with NGC 524 (Brough et al. 2006). The total environmental halo mass is approximately  $10^{13} M_{\odot}$ , based on the total GC numbers of NGC 524 itself (Harris et al. 2013; Burkert & Forbes 2020). MATLAS-42 is thus not in as dense an environment as those UDGs found in clusters, and the expected environmental enhancement to GC formation is not expected to be large.

Thus far, we have largely assumed that both the ‘bluer’ and ‘redder’ populations of star clusters around MATLAS-42 are GCs. It is possible that one of the GC subpopulations is not old bona fide GCs (and hence  $N_{GC}$  is overestimated) but rather that it is comprised of young clusters with an age similar to the galaxy itself. If these young clusters share the galaxy’s metallicity, then they are likely to have blue colours. The old bona fide GCs would thus consist of only the red subpopulation, and  $N_{GC}$  would be reduced to around a dozen. The implication of the red subpopulation being the bona fide GCs is

that there would have to be a large population of metal-rich GCs - more than what is traditionally seen for dwarf galaxies, where such metal-rich clusters are outliers in the underlying population (see e.g., the dwarf galaxy GC colour distributions in Fielder et al. 2024, fig. 7). Should these metal-rich clusters be confirmed for MATLAS-42, and/or further UDGs be found with significant populations of metal-rich GCs, it would be worthwhile to add this puzzle to the menagerie of oddities thus far discovered in UDG GC systems.

Even with a revision of the GC system downward to exclude a possible young star cluster population, MATLAS-42 would still be relatively GC-rich for its stellar mass. For example, Marleau et al. (2025) found that only  $\sim 1/4$  of the 1100 dwarf galaxy candidates in their EUCLID observations of the Perseus cluster had  $>2$  GC candidates. Furthermore, we reiterate that of the 74 dwarf galaxies studied by Marleau et al. (2024) using the same methods, MATLAS-42 was clearly one of the most GC-rich, with 64% of their galaxies shown to have few, if any, GCs. In having a dozen ‘bona-fide’ GCs it would still be GC-rich within their sample and any formation scenario for MATLAS-42 would need to explain both star cluster populations.

GAMA 526784 (Buzzo et al. 2025b) is similar to MATLAS-42 in that it exhibits two populations of star clusters, it has a gas reservoir, and it has been shown to have both an underlying old, quiescent stellar body, along with signs of recent star formation. Indeed, both galaxies show evidence of two components in their stellar body (Marleau et al. 2024; Buzzo et al. 2025b). While MATLAS-42 exhibited the majority of its star formation a few Gyr ago, for GAMA 526784, the period of its significant star formation was much more recent, with many of the star clusters having ages  $<1$  Gyr. Buzzo et al. (2025b) posited that an established galaxy may experience localised cluster formation caused by gas instabilities, which are themselves the result of gravitational interactions from nearby companions. For MATLAS-42, this scenario seems entirely plausible.

However, galaxies can (and do) form stars without external triggering. For example, there is also the case of the ‘Disco Ball’ Galaxy (Khim et al. 2025). This UDG hosts a significant population of star clusters ( $34 \pm 11$ ) and shows signs of recent star formation activity, despite being on the red sequence. Its nearest spectroscopically confirmed neighbour is 1.7 Mpc away, suggesting that this recent star formation must not be triggered externally (Khim et al. 2025). It is currently unclear what the major driving processes are in the formation of the ‘Disco Ball’.

To best understand the reignition of star formation in MATLAS-42:

- (i) Resolved HI and molecular gas observations would allow for an investigation into the distribution of its gas content, along with how it is turning its neutral gas into molecular gas for star formation.
- (ii) Deep spectroscopy targeting the ages and metallicities of individual star clusters around MATLAS-42 would help us better understand its star formation history. This would also aid in understanding the nature of its underlying ‘bluer’ star cluster population.

### 3.3 Time Evolution of the GC system

Despite it being clear that MATLAS-42 has not formed and evolved via a similar pathway to the older, quenched, GC-rich UDGs, it might be tempting to perceive it as an analogue to how these UDGs may have looked at earlier times. To assess this, in Figure 6 we build a toy model for the passive evolution of the GC-to-stellar mass ratio  $M_{GC}/M_{\star}$  with time (a similar quantity of GC specific mass,  $S_{M}$ , is used in the literature; Miller & Lotz 2007; Peng et al. 2008). In the top panel, we show the passive evolution of stellar mass with

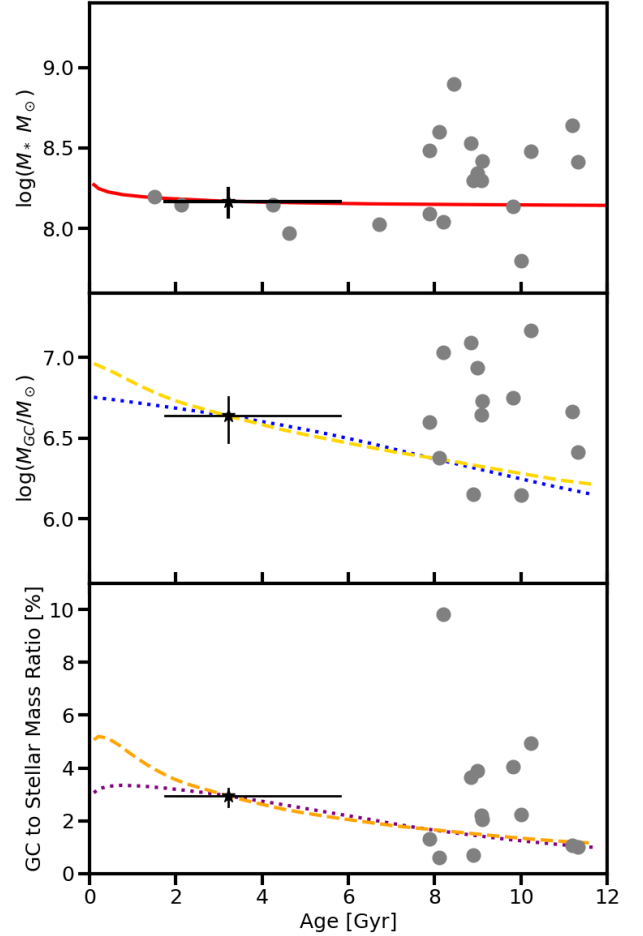


**Figure 6.** A toy model for the possible evolution of the GC to stellar mass ratio of MATLAS-42. In all panels, we plot MATLAS-42 (black star) along with UDGs from the catalogue of Gannon et al. (2024b) with GC information (grey points). *Top panel:* Stellar mass vs. age. We include the model for the mass loss of a passively evolving Kroupa (2001) IMF-based stellar population from the review of Courteau et al. (2014) as a red line. *Middle panel:* Total GC system mass vs. age. We include two models of GC system mass loss in time based on the simulations of Moreno-Hilario et al. (2024). In blue (dotted line), we plot the median mass loss evolution coming from their galaxy ‘A’ simulation, while in yellow (dashed line), we plot the median mass loss evolution coming from their galaxy ‘D’ simulation. *Lower panel:* GC to stellar mass ratio vs. age. As this panel represents a ratio of the two panels above it, we combine the evolutionary curves from above for this panel. That is, the orange dashed curve is a combination of the red and yellow curves above, while the purple dotted curve is a combination of the red and blue above. When combining, the stellar mass lost in the GC system is gained by the stellar body of the galaxy. MATLAS-42 is plotted using our spectroscopic age, the stellar mass derived by Buzzo et al. (2024), and a total GC system mass calculated using the GC counts of Marleau et al. (2024), assuming an average GC mass of  $2 \times 10^5 M_{\odot}$ . We conclude that while MATLAS-42 exhibits a rich GC system at the present day, this will decay with time. If it passively evolves, in  $\sim 7$  Gyr time (i.e., when it will be  $\sim 10$  Gyrs old similar to old UDGs), it will only have a GC system representing  $\sim 1\%$  of its stellar mass. It is thus likely not a low redshift analogue of a ‘failed galaxy’ progenitor.

time from the Kroupa (2001) IMF models shown in the galaxy mass review of Courteau et al. (2014). As galaxies passively evolve, stellar mass is slowly lost to stellar evolution. In the middle panel, we show the passive evolution of GC system mass from the simulations of Moreno-Hilario et al. (2024). As GC systems passively evolve, individual GCs slowly evaporate and are disrupted, decreasing the total mass within the GC system. In this panel, we show two evolutionary curves from their galaxies ‘A’ and ‘D’, which encapsulate the variation of GC system mass evolution in their simulations. These galaxies also bracket the extremities of dynamical masses known for UDGs ( $\sim 10^9 - 10^{11} M_{\odot}$ ), with their galaxy ‘E’ having a greater dynamical mass than has been measured in UDGs ( $> 10^{11} M_{\odot}$ ). In the bottom panel, we show the evolution of  $M_{GC}/M_{\star}$  with time. We create this toy model by combining the evolutionary curves of the above two panels, accounting for the fact that mass lost by the GC system is gained by the stellar body of the galaxy. Based on our toy model, we have a general expectation that the  $M_{GC}/M_{\star}$  ratio will slowly decrease with time for a passively evolving system.

In terms of MATLAS-42, the implication is that its current ratio of  $M_{GC}/M_{\star} = 2.9\%$  for a galaxy that is 3.2 Gyr old will decrease to below 1% within 7 Gyr. Put another way, if MATLAS-42 were to evolve passively until its mass-weighted age was 10 Gyr, as is the case for many of the quenched, GC-rich UDGs studied spectroscopically, it would have a noticeably lower  $M_{GC}/M_{\star}$  than they. Indeed, there are multiple UDGs in the Gannon et al. (2024b) catalogue that have  $M_{GC}/M_{\star} > 5\%$ . Given that our toy model demonstrates this ratio decreases with passive evolution, it is not possible to easily evolve MATLAS-42 into these systems with time. We conclude that MATLAS-42 should not be interpreted as a low redshift analogue of GC-rich UDGs’ progenitors.

An assumption of our toy model is that there is no subsequent star formation within the galaxy. As MATLAS-42 currently contains HI-gas it is likely that this assumption is poor. Any subsequent star formation will form new stars; however, the star formation would also be expected to form GCs very inefficiently compared to star formation events at high-redshift, where the vast majority of GCs in the Universe have formed. Our toy model thus represents an upper limit of the evolution of  $M_{GC}/M_{\star}$  with time, with most future star formation generally expected to cause  $M_{GC}/M_{\star}$  to drop.

A second assumption of our toy model is that the GC system of the galaxy is as young as the galaxy itself (i.e., 3.2 Gyr old), making it likely that they are younger star clusters than what is traditionally called a GC. Given that much of the mass loss of a GC system occurs when it is young, the star clusters that have ages more typical for a GC ( $\sim 12$  Gyrs) will experience less mass loss than our model suggests, possibly causing less decay in  $M_{GC}/M_{\star}$  than is modelled. However, as we have measured an age older than  $\sim 2$  Gyr we are beyond the point where much of the mass loss occurs for young star clusters. After this point the mass loss rate is relatively constant for either model. We suggest that this assumption has little impact on our results.

We reiterate the general conclusions of this subsection: 1) That our modelling suggests galaxies’  $M_{GC}/M_{\star}$  is generally expected to decline with time and 2) that MATLAS-42 is not a low redshift analogue of what a “failed galaxy” progenitor looked like at high redshift. It is not sufficiently GC-rich for this to be the case. At most, it may have formed similar to a “failed galaxy” but has recently rejuvenated star formation.

## 4 CONCLUSIONS

In this work, we have studied the recessional velocity, stellar population and GC-population of the GC-rich, gas-rich, group UDG, MATLAS-42 using spectroscopic data from the Keck Telescopes. Our conclusions are as follows:

- We measure a recessional velocity of  $2433 \pm 8 \text{ km s}^{-1}$  for MATLAS-42, confirming its association with the NGC 502 group and with the HI-gas previously assumed to have been associated with it. Confirmation of its environment/distance confirms its status as a UDG.
- We measure a mass-weighted age of  $3.2^{+2.6}_{-1.5}$  Gyr and a mass-weighted metallicity of  $[M/H] = -1.19^{+0.42}_{-0.30}$  dex. This places MATLAS-42 at the lower, metal-poor edge of the regular mass-metallicity relationship for dwarf galaxies. It also places MATLAS-42 as being significantly younger than any other GC-rich UDG previously studied with spectroscopy.
- When considering established formation pathways and previously observed UDGs in low-density environments, we do not find an obvious formation pathway for MATLAS-42 and its rich GC system. Namely, it cannot be a simple “failed galaxy” as it has recently experienced star formation and is not quenched - a requirement of the formation pathway. If it formed via this pathway, it has now diverged from it. Further, its rich GC system cannot be explained by ‘biasing’ as it does not reside in a particularly dense environment.
- Finally, we build a toy model of the evolution of  $M_{GC}/M_{\star}$ . We find that its current  $M_{GC}/M_{\star} = 2.9\%$  will evolve to  $< 1\%$  in 7 Gyr of passive evolution. As such, MATLAS-42 cannot be a low redshift analogue of the progenitors of the previously studied quenched, GC-rich UDGs.

To best understand the galaxy further, measurements of its star formation history and gas content (to see when it rejuvenated) are required. Deep spectroscopy of its star cluster system would also help to disentangle the nature of its blue and red populations of star clusters.

## ACKNOWLEDGMENTS

We thank the anonymous referee for their work to improve the quality and clarity of this paper. DAF and JPB thank the ARC for financial support via DP220101863. AJR was supported by National Science Foundation grant AST-2308390. A.F.M. has received support from RYC2021-031099-I and PID2021-123313NA-I00 of MICIN/AEI/10.13039/501100011033/FEDER, UE, NextGenerationEU/PRT. Some of the data presented herein were obtained at Keck Observatory, which is a private 501(c)3 non-profit organization operated as a scientific partnership among the California Institute of Technology, the University of California, and the National Aeronautics and Space Administration. The Observatory was made possible by the generous financial support of the W. M. Keck Foundation. The authors wish to recognize and acknowledge the very significant cultural role and reverence that the summit of Maunakea has always had within the Native Hawaiian community. We are most fortunate to have the opportunity to conduct observations from this mountain.

## DATA AVAILABILITY

This data makes use of data from the Keck Telescopes which is available on the Keck Observatory Archive 18 months after the date of its observations. Per the request of Gannon et al. (2024b), we thank

the following authors for their contribution to the catalogue [McConnachie \(2012\)](#); [van Dokkum et al. \(2015\)](#); [Beasley et al. \(2016\)](#); [Martin et al. \(2016\)](#); [Yagi et al. \(2016\)](#); [Martínez-Delgado et al. \(2016\)](#); [van Dokkum et al. \(2016, 2017\)](#); [Karachentsev et al. \(2017\)](#); [van Dokkum et al. \(2018\)](#); [Toloba et al. \(2018\)](#); [Gu et al. \(2018\)](#); [Lim et al. \(2018\)](#); [Ruiz-Lara et al. \(2018\)](#); [Alabi et al. \(2018\)](#); [Ferré-Mateu et al. \(2018\)](#); [Forbes et al. \(2018\)](#); [Martín-Navarro et al. \(2019\)](#); [Chilingarian et al. \(2019\)](#); [Fensch et al. \(2019\)](#); [Danieli et al. \(2019\)](#); [van Dokkum et al. \(2019\)](#); [Torrealba et al. \(2019\)](#); [Iodice et al. \(2020\)](#); [Collins et al. \(2020\)](#); [Müller et al. \(2020\)](#); [Gannon et al. \(2020\)](#); [Lim et al. \(2020\)](#); [Müller et al. \(2021\)](#); [Forbes et al. \(2021\)](#); [Shen et al. \(2021b\)](#); [Ji et al. \(2021\)](#); [Huang & Kaposov \(2021\)](#); [Gannon et al. \(2021, 2022\)](#); [Mihos et al. \(2022\)](#); [Danieli et al. \(2022\)](#); [Villaume et al. \(2022\)](#); [Webb et al. \(2022\)](#); [Saifollahi et al. \(2022\)](#); [Janssens et al. \(2022\)](#); [Gannon et al. \(2023\)](#); [Ferré-Mateu et al. \(2023\)](#); [Toloba et al. \(2023\)](#); [Iodice et al. \(2023\)](#); [Shen et al. \(2023\)](#); [Janssens et al. \(2024\)](#); [Gannon et al. \(2024a\)](#); [Buttitta et al. \(2025\)](#).

## REFERENCES

- Alabi A., et al., 2018, *MNRAS*, **479**, 3308
- Amorisco N. C., Monachesi A., Agnello A., White S. D. M., 2018, *MNRAS*, **475**, 4235
- Beasley M. A., Romanowsky A. J., Pota V., Navarro I. M., Martínez Delgado D., Neyer F., Deich A. L., 2016, *ApJ*, **819**, L20
- Brough S., Forbes D. A., Kilborn V. A., Couch W., 2006, *MNRAS*, **370**, 1223
- Burkert A., Forbes D. A., 2020, *AJ*, **159**, 56
- Buttitta C., et al., 2025, *A&A*, **694**, A276
- Buzzo M. L., et al., 2024, *MNRAS*, **529**, 3210
- Buzzo M. L., et al., 2025a, *MNRAS*, **536**, 2536
- Buzzo M. L., Hilker M., Zanella A., Fahrion K., McDermid R. M., van der Burg R., Mirabile M., 2025b, *A&A*, **699**, A94
- Cappellari M., 2017, *MNRAS*, **466**, 798
- Cappellari M., 2023, *MNRAS*, **526**, 3273
- Cappellari M., Emsellem E., 2004, *PASP*, **116**, 138
- Cappellari M., et al., 2011, *MNRAS*, **413**, 813
- Carleton T., Errani R., Cooper M., Kaplinghat M., Peñarrubia J., Guo Y., 2019, *MNRAS*, **485**, 382
- Chan T. K., Kereš D., Wetzell A., Hopkins P. F., Faucher-Giguère C. A., El-Badry K., Garrison-Kimmel S., Boylan-Kolchin M., 2018, *MNRAS*, **478**, 906
- Chilingarian I. V., Afanasiev A. V., Grishin K. A., Fabricant D., Moran S., 2019, *ApJ*, **884**, 79
- Collins M. L. M., Tollerud E. J., Rich R. M., Ibata R. A., Martín N. F., Chapman S. C., Gilbert K. M., Preston J., 2020, *MNRAS*, **491**, 3496
- Courteau S., et al., 2014, *Reviews of Modern Physics*, **86**, 47
- Danieli S., van Dokkum P., Conroy C., Abraham R., Romanowsky A. J., 2019, *ApJ*, **874**, L12
- Danieli S., et al., 2022, *ApJ*, **927**, L28
- Di Cintio A., Brook C. B., Dutton A. A., Macciò A. V., Obreja A., Dekel A., 2017, *MNRAS*, **466**, L1
- Fensch J., et al., 2019, *A&A*, **625**, A77
- Ferré-Mateu A., et al., 2018, *MNRAS*, **479**, 4891
- Ferré-Mateu A., Gannon J. S., Forbes D. A., Buzzo M. L., Romanowsky A. J., Brodie J. P., 2023, *MNRAS*, **526**, 4735
- Ferré-Mateu A., Gannon J., Forbes D. A., Romanowsky A. J., Buzzo M. L., Brodie J. P., 2025, *A&A*, **694**, L6
- Fielder C., Jones M. G., Sand D. J., Bennet P., Crnojević D., Karunakaran A., Mutlu-Pakdil B., Spekkens K., 2024, *AJ*, **168**, 212
- Forbes D. A., Gannon J., 2024, *MNRAS*, **528**, 608
- Forbes D. A., Gannon J. S., 2025, *MNRAS*, **543**, L1
- Forbes D. A., Read J. I., Gieles M., Collins M. L. M., 2018, *MNRAS*, **481**, 5592
- Forbes D. A., Gannon J., Couch W. J., Iodice E., Spavone M., Cantiello M., Napolitano N., Schipani P., 2019, *A&A*, **626**, A66
- Forbes D. A., Alabi A., Romanowsky A. J., Brodie J. P., Arimoto N., 2020, *MNRAS*, **492**, 4874
- Forbes D. A., Gannon J. S., Romanowsky A. J., Alabi A., Brodie J. P., Couch W. J., Ferré-Mateu A., 2021, *MNRAS*, **500**, 1279
- Forbes D. A., et al., 2023, *MNRAS*, **525**, L93
- Forbes D. A., Buzzo M. L., Ferré-Mateu A., Romanowsky A. J., Gannon J., Brodie J. P., Collins M. L. M., 2025, *MNRAS*, **536**, 1217
- Gannon J. S., Forbes D. A., Romanowsky A. J., Ferré-Mateu A., Couch W. J., Brodie J. P., 2020, *MNRAS*, **495**, 2582
- Gannon J. S., et al., 2021, *MNRAS*, **502**, 3144
- Gannon J. S., et al., 2022, *MNRAS*, **510**, 946
- Gannon J. S., Forbes D. A., Brodie J. P., Romanowsky A. J., Couch W. J., Ferré-Mateu A., 2023, *MNRAS*, **518**, 3653
- Gannon J. S., et al., 2024a, *MNRAS*, **531**, 1789
- Gannon J. S., Ferré-Mateu A., Forbes D. A., Brodie J. P., Buzzo M. L., Romanowsky A. J., 2024b, *MNRAS*, **531**, 1856
- Gannon J. S., Kimmig L. C., Forbes D. A., Brodie J. P., Valenzuela L. M., Remus R.-S., Pfeffer J. L., Dolag K., 2025, *The Open Journal of Astrophysics*, **8**, E150
- Graham A. W., Driver S. P., 2005, *Publ. Astron. Soc. Australia*, **22**, 118
- Gu M., et al., 2018, *ApJ*, **859**, 37
- Haacke L., et al., 2025, *arXiv e-prints*, p. arXiv:2504.03132
- Habas R., et al., 2020, *MNRAS*, **491**, 1901
- Harris W. E., Harris G. L. H., Alessi M., 2013, *ApJ*, **772**, 82
- Haynes M. P., et al., 2018, *ApJ*, **861**, 49
- Heesters N., et al., 2023, *A&A*, **676**, A33
- Huang K.-W., Kaposov S. E., 2021, *MNRAS*, **500**, 986
- Iodice E., et al., 2020, *A&A*, **635**, A3
- Iodice E., et al., 2023, *A&A*, **679**, A69
- Ivleva A., Remus R.-S., Valenzuela L. M., Dolag K., 2024, *A&A*, **687**, A105
- Janssens S. R., et al., 2022, *MNRAS*, **517**, 858
- Janssens S. R., et al., 2024, *MNRAS*, **534**, 783
- Ji A. P., et al., 2021, *ApJ*, **921**, 32
- Jiang F., Dekel A., Freundlich J., Romanowsky A. J., Dutton A. A., Macciò A. V., Di Cintio A., 2019, *MNRAS*, **487**, 5272
- Jones M. G., et al., 2023, *ApJ*, **942**, L5
- Karachentsev I. D., Makarova L. N., Sharina M. E., Karachentseva V. E., 2017, *Astrophysical Bulletin*, **72**, 376
- Keim M. A., et al., 2025, *arXiv e-prints*, p. arXiv:2506.10220
- Khim D. J., Zaritsky D., Sandoval Ascencio L., Cooper M. C., Donnerstein R., 2025, *ApJ*, **989**, 154
- Kirby E. N., Cohen J. G., Guhathakurta P., Cheng L., Bullock J. S., Gallazzi A., 2013, *ApJ*, **779**, 102
- Kroupa P., 2001, *MNRAS*, **322**, 231
- Lee J., Shin E.-j., Kim J.-h., 2021, *ApJ*, **917**, L15
- Lee J., Shin E.-j., Kim J.-h., Shapiro P. R., Chung E., 2024, *ApJ*, **966**, 72
- Li D. D., et al., 2025, *ApJ*, **984**, 147
- Liao S., et al., 2019, *MNRAS*, **490**, 5182
- Lim S., Peng E. W., Côté P., Sales L. V., den Brok M., Blakeslee J. P., Guhathakurta P., 2018, *ApJ*, **862**, 82
- Lim S., et al., 2020, *ApJ*, **899**, 69
- Ma X., Hopkins P. F., Faucher-Giguère C.-A., Zolman N., Muratov A. L., Kereš D., Quataert E., 2016, *MNRAS*, **456**, 2140
- Marleau F. R., et al., 2021, *A&A*, **654**, A105
- Marleau F. R., et al., 2024, *A&A*, **690**, A339
- Marleau F. R., et al., 2025, *A&A*, **697**, A12
- Martín-Navarro I., et al., 2019, *MNRAS*, **484**, 3425
- Martin N. F., et al., 2016, *ApJ*, **833**, 167
- Martin G., et al., 2019, *MNRAS*, **485**, 796
- Martínez-Delgado D., et al., 2016, *AJ*, **151**, 96
- McConnachie A. W., 2012, *AJ*, **144**, 4
- Mihos J. C., et al., 2022, *ApJ*, **924**, 87
- Miller B. W., Lotz J. M., 2007, *ApJ*, **670**, 1074
- Moreno-Hilario E., Martínez-Medina L. A., Li H., Souza S. O., Pérez-Villegas A., 2024, *MNRAS*, **527**, 2765
- Morrissey P., et al., 2018, The Keck Cosmic Web Imager Integral Field Spectrograph ([arXiv:1807.10356](#)), doi:10.3847/1538-4357/aad597
- Müller O., et al., 2020, *A&A*, **640**, A106

Müller O., et al., 2021, *ApJ*, 923, 9  
 Peng E. W., Lim S., 2016, *ApJ*, 822, L31  
 Peng E. W., et al., 2008, *ApJ*, 681, 197  
 Pietrinferni A., et al., 2021, *ApJ*, 908, 102  
 Poulain M., et al., 2021, *MNRAS*, 506, 5494  
 Poulain M., et al., 2022, *A&A*, 659, A14  
 Remus R.-S., Forbes D. A., 2022, *ApJ*, 935, 37  
 Ruiz-Lara T., et al., 2018, *MNRAS*, 478, 2034  
 Saifollahi T., Zaritsky D., Trujillo L., Peletier R. F., Knapen J. H., Amorisco N., Beasley M. A., Donnerstein R., 2022, *MNRAS*, 511, 4633  
 Saifollahi T., et al., 2025, *A&A*, 703, A184  
 Sales L. V., Navarro J. F., Peñafiel L., Peng E. W., Lim S., Hernquist L., 2020, *MNRAS*, 494, 1848  
 Shen Z., van Dokkum P., Danieli S., 2021a, *ApJ*, 909, 179  
 Shen Z., et al., 2021b, *ApJ*, 914, L12  
 Shen Z., van Dokkum P., Danieli S., 2023, arXiv e-prints, p. arXiv:2309.08592  
 Silk J., 2019, *MNRAS*, 488, L24  
 Somalwar J. J., Greene J. E., Greco J. P., Huang S., Beaton R. L., Goulding A. D., Lancaster L., 2020, *ApJ*, 902, 45  
 Tang Y., et al., 2025, *ApJ*, 978, 21  
 Toloba E., et al., 2018, *ApJ*, 856, L31  
 Toloba E., et al., 2023, arXiv e-prints, p. arXiv:2305.06369  
 Torrealba G., et al., 2019, *MNRAS*, 488, 2743  
 Trujillo-Gomez S., Kruijssen J. M. D., Reina-Campos M., 2022, *MNRAS*, 510, 3356  
 Vazdekis A., et al., 2015, *MNRAS*, 449, 1177  
 Villaume A., et al., 2022, *ApJ*, 924, 32  
 Webb K. A., et al., 2022, *MNRAS*, 516, 3318  
 West M. J., 1993, *MNRAS*, 265, 755  
 Wright A. H., et al., 2017, *MNRAS*, 470, 283  
 Yagi M., Koda J., Komiyama Y., Yamanoi H., 2016, *ApJS*, 225, 11  
 Zaritsky D., et al., 2019, *ApJS*, 240, 1  
 Zaritsky D., Donnerstein R., Dey A., Karunakaran A., Kadowaki J., Khim D. J., Spekkens K., Zhang H., 2023, *ApJS*, 267, 27  
 van Dokkum P. G., Abraham R., Merritt A., Zhang J., Geha M., Conroy C., 2015, *ApJ*, 798, L45  
 van Dokkum P., et al., 2016, *ApJ*, 828, L6  
 van Dokkum P., et al., 2017, *ApJL*, 844, L11  
 van Dokkum P., et al., 2018, *Nature*, 555, 629  
 van Dokkum P., et al., 2019, *ApJ*, 880, 91  
 van Dokkum P., et al., 2022, *Nature*, 605, 435

## APPENDIX A: PPF CONSISTENCY CHECKS

As discussed in the main body of the text, while our bootstrapping of the spectra was able to derive a relatively stable age and metallicity for MATLAS-42 we were unable to derive a stable star formation history. We show our results for these fits in Figures A1. We find that the mass-weighted ages and metallicities are well-constrained. In order to test if our choice of fitting parameters greatly affected our results, we performed multiple different realisations of the spectra fitting. Namely, we refitted the spectra using combinations of with/without emission-line gas templates, 5th/10th/15th order multiplicative polynomials, adding in pPXF's regularisation parameter as 0.01/0.05/0.1/0.5, and 7 different options of which regions of the spectra we masked. In all cases, ages were within our uncertainties. In nearly all cases, metallicities were within joint  $1-\sigma$  uncertainties with a slight bias to many realisations measuring MATLAS-42 to be slightly more metal-rich. Overall, the conclusions we draw in our paper would not be significantly affected were we to have chosen any of these consistency check bootstrap fits instead of our fiducial results. Finally, none of these tests resulted in well-constrained star formation histories. We conclude that, due to the young stellar population dominating much of the light in our spectrum, it is difficult to

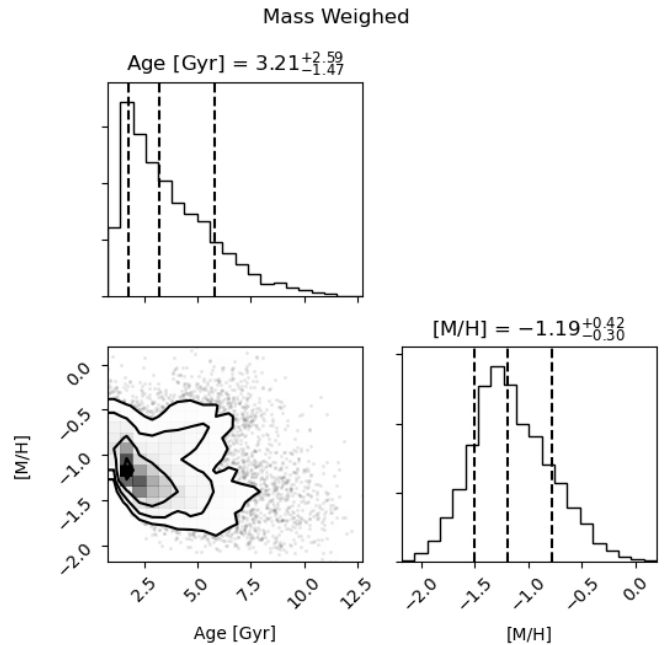


**Figure A1.** The mass-weighted results of our 10000 bootstrap fits of the spectrum. Ages and metallicities are relatively well-constrained by the data.

accurately assess the exact properties of the underlying older stellar population. As such, we do not include any discussion of the star formation history of MATLAS-42 in this work beyond taking note of it experiencing recent, significant star formation, and solely focus on its age and metallicity.

This paper has been typeset from a  $\text{\TeX}/\text{\LaTeX}$  file prepared by the author.